

Temporal Logic Motion Planning with Convex Optimization via Graphs of Convex Sets

Vince Kurtz *Student Member, IEEE* and Hai Lin *Senior Member, IEEE*

Abstract—Temporal logic is a concise way of specifying complex tasks. But motion planning to achieve temporal logic specifications is difficult, and existing methods struggle to scale to complex specifications and high-dimensional system dynamics. In this paper, we cast Linear Temporal Logic (LTL) motion planning as a shortest path problem in a Graph of Convex Sets (GCS) and solve it with convex optimization. This approach brings together the best of modern optimization-based temporal logic planners and older automata-theoretic methods, addressing the limitations of each: we avoid clipping and passthrough by representing paths with continuous Bezier curves; computational complexity is polynomial (not exponential) in the number of sample points; global optimality can be certified (though it is not guaranteed); soundness and probabilistic completeness are guaranteed under mild assumptions; and most importantly, the method scales to complex specifications and high-dimensional systems, including a 30-DoF humanoid. Open-source code is available at https://github.com/vincekurtz/ltl_gcs.

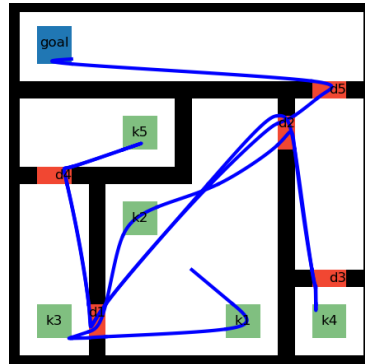
I. INTRODUCTION

Robotic and cyber-physical systems often need to do more than avoid obstacles or regulate around a set point. To this end, temporal logics like Linear Temporal Logic (LTL), Metric Temporal Logic (MTL), and Signal Temporal Logic (STL) have grown in popularity as a compact means of expressing complex control objectives. Beyond being both expressive and concise, they are relatively easy for humans to understand, with a combination of familiar boolean operators (“and”, “or”, “not”) and temporal operators with intuitive names (“next”, “always”, “eventually”). The usefulness of temporal logic becomes most obvious in scenarios like that shown in Fig. 1a, where a mobile robot may not pass through a door (red) *until* it has picked up a corresponding key (green) and must *eventually* reach a goal (blue).

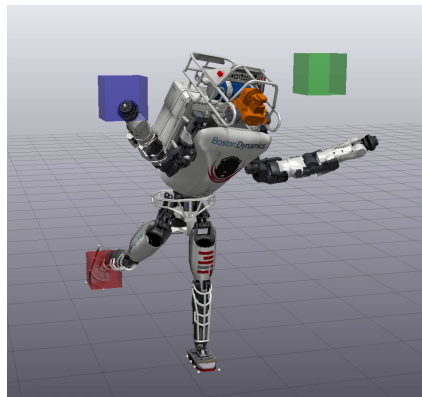
Temporal logic motion planning is a fundamentally difficult (NP-hard) problem, and is especially challenging for high degree-of-freedom (DoF) systems. The current state-of-the-art is to use Mixed-Integer Convex Programming (MICP) [1]. The MICP approach is sound and complete (it will always find the optimal solution if

The support of the National Science Foundation (Grant No. CNS-1830335, IIS-2007949) is gratefully acknowledged.

Vince Kurtz and Hai Lin are both with the Electrical Engineering Department, University of Notre Dame, Notre Dame, IN, USA.



(a) A benchmark from [3], where a mobile robot must pick up keys (k_1, k_2, \dots) before passing through doors (d_1, d_2, \dots) and reach a goal. The fastest reported solve time is **49.5 seconds** for a piecewise-linear solution [4]. Our proposed approach finds a C^2 globally optimal solution in **5.8 seconds**.



(b) A 30-DoF humanoid is tasked with touching the green target with its left hand, then the red target with its right foot, then the blue target with its right hand. Convex optimization finds a smooth configuration-space solution in under 10 seconds.

Fig. 1: Our proposed approach scales to both complex task specifications (a) and high-dimensional systems (b).

a solution exists) but it has some significant drawbacks. In particular, standard MICP encodings introduce binary variables for each subformula at each time step. Since the worst-case complexity of MICP is exponential in the number of binary variables, MICP scales poorly with both specification complexity and the number of sample points used to represent a path [1, 2].

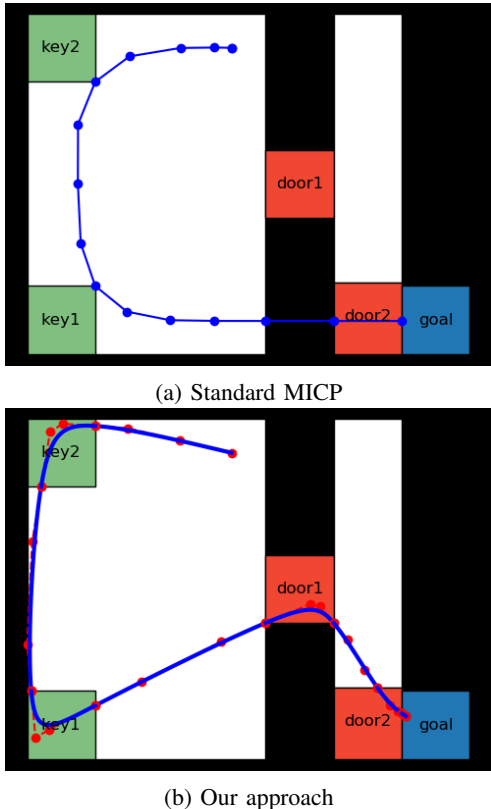


Fig. 2: A mobile robot must pick up two keys before it can pass through corresponding doors to reach a goal region, as encoded in formula (10). A standard MICP (2a) uses a fixed discretization of time, leading to a path that passes through an obstacle. Our proposed approach (2b) considers all values along a smooth Bezier spline, avoiding clipping and pass-through.

The discretization of time used in standard MICP encodings compounds this problem. A coarse discretization gives rise to “clipping”, where the path may intersect with obstacles between timesteps, violating the specification. An example of this is shown in Fig. 2a. Clipping can be mitigated with a finer discretization, but this increases computational cost exponentially [1].

While exponential cost with the specification complexity is inevitable given the NP-hardness of the problem, it is less clear whether exponential cost with the number of sample points is also inevitable. Intuitively, planning to achieve the same specification with a finer discretization does not seem to make the problem fundamentally harder. Indeed, we show that this exponential complexity can be avoided: our proposed approach scales polynomially with the number of sample points.

Our key idea is to re-frame LTL motion planning as a shortest path problem in a Graph of Convex Sets (GCS) [5]. This results in an MICP with a very tight convex

relaxation—so tight, in fact, that it can often be solved to global optimality with convex optimization and rounding [6]. Even if the approximate solution to this MICP is sub-optimal (bounds on sub-optimality are available [6] and convex optimization often finds the globally optimal solution in practice), any integer-feasible solution is guaranteed to satisfy the specification.

Our proposed approach scales well to complex specifications and high-dimensional configuration spaces, outperforming the state-of-the-art on numerous benchmark problems (see Section VII). Furthermore, we parameterize motion plans with Bezier splines, allowing us to design smooth paths without clipping or pass-through.

Our primary contributions are summarized as follows:

- We show that LTL motion planning can be formulated as a shortest path problem in a GCS and solved efficiently using convex programming.
- By representing paths with smooth Bezier splines, we avoid the clipping and pass-through problems associated with most discrete-time temporal logic formulations.
- Our proposed approach scales polynomially with the number of control points used to represent a smooth path, in contrast with the exponential complexity of standard methods.
- We provide proofs of soundness and probabilistic completeness.
- We demonstrate the scalability of our proposed approach to complex specifications and high-dimensional configuration spaces with several simulation examples, and provide open-source code to reproduce these results [7].

The remainder of this paper is organized as follows: Section II reviews related work on temporal logic motion planning. A formal problem statement and relevant definitions are given in Section III. Background information on Bezier curves and graphs of convex sets is given in Section IV. Our main result—a convex programming solution to temporal logic motion planning—is described in Section V. Section VI provides proofs of the soundness, completeness, and computational complexity of our proposed approach. We provide examples in Section VII, discuss limitations of our proposed method in Section VIII, and conclude with Section IX.

II. RELATED WORK

Early work on temporal-logic-based control was dominated by automata-theoretic methods [3, 8]. These methods generally assume that the system can be modeled as a finite-state transition system. Once a given LTL formula is transformed into an equivalent automaton, a simple graph search in the product of the transition system and the automaton reveals a satisfying path

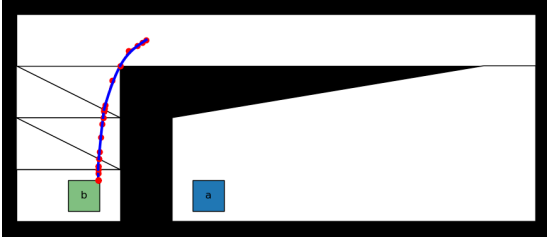


Fig. 3: A mobile robot is tasked with eventually reaching region a (blue) or region b (green), as denoted by formula (9). Standard abstraction-based methods would likely take the longer path to a , since this requires passing through fewer regions. Our proposed approach finds the shorter path to b directly.

[8, Chapter 5]. For finite-state transition systems, such automata-based methods are sound, complete, and computationally efficient. Similar techniques have achieved widespread adoption in formal verification and model checking applications [9].

Applying automata-based methods to motion planning is non-trivial, as we must plan in (non-finite) configuration space. The dominant idea in the literature is to use some sort of finite transition system abstraction [3, 10, 11], typically related to labeled regions in configuration space. Once a satisfying abstract path is found, a lower-level motion planner searches for a path through the corresponding regions. While this can be computationally efficient, as it separates logical constraints from physical dynamics, it is difficult to account for the gap between the geometry of the scenario and the abstract transition system. In practice, this means that an abstract path may be dynamically infeasible or inefficient once it is translated to a motion plan: shortest paths in the abstraction do not necessarily correspond to shortest paths in configuration space, as illustrated in Fig. 3.

In prior work, we sought to address this gap with a Counter Example Guided Inductive Synthesis (CEGIS) [12] inspired cycle of planning and re-planning for both a high-level automata-based planner and a low-level motion planner [10, 11]. While this allows for completeness guarantees, even local optimality is difficult to achieve and many re-planning cycles may be required.

Another drawback for many automata-based methods stems from a reliance on sampling-based motion planning [10, 13, 14, 15]. While such methods can have good scalability properties, they often struggle on problems with narrow passages [16] and it is difficult to enforce dynamic feasibility. It is also often difficult to tell whether a specification is infeasible, as sampling-based methods do not provide certificates of infeasibility.

A particularly interesting set of automata-based planners do not search for specific satisfying paths, but rather

generate feedback controllers that guarantee closed-loop satisfaction of the specification [17, 18]. While these methods provide an elegant way to bridge the gap between continuous dynamics and the discrete specification, their scalability is limited by the fact that they search for solutions across the whole state space. To the best of our knowledge, such techniques have not been able to scale beyond 4-dimensional state spaces.

Despite these limitations, we are strongly inspired by automata-theoretic methods in this paper. Specifically, we use the GCS framework to perform graph search in the product of a transition system and an automaton. In contrast to existing abstraction-based methods, this graph search accounts for the geometry of the scenario directly, avoiding the need for separate low-level and high-level planners. Unlike sampling-based methods, our GCS method can navigate narrow passages with ease and enforce dynamical feasibility for differentially flat systems [19]. Unlike methods that search for feedback controllers, our approach scales to high-dimensional systems, including a 30-DoF humanoid.

Optimization-based methods using mixed-integer programming were developed to address the limitations of abstraction-based methods [1]. MICP methods typically do not require any abstraction, and consider the state (or configuration) space directly. Continuous variables represent the state at discrete time steps along the path. Binary variables and additional constraints are added to enforce the specification [20, 1]. The MICP approach is sound, complete, and (unlike automata-based methods) allows for guarantees of global optimality. MICP is particularly popular for STL [20, 2], but has also been applied to LTL [21], MTL [2], and a variety of other temporal logics. MICP is widely considered to be the state-of-the-art in temporal logic motion planning [1].

Nonetheless, MICP methods have some significant limitations. New binary variables are introduced for each subformula (or predicate) for each time step. This means that the computational complexity is exponential not only in the size of the formula, but also in the number of time steps. Making matters worse, too few timesteps can lead to clipping and pass-through problems, where the path intersects obstacles between timesteps (Fig. 2a).

Mitigating these limitations is an area of much active research. [22] uses a control-barrier function between time steps to avoid clipping and pass-through. [23] and [24] reduce the size of the MICP, but are still left with exponential complexity in the number of time steps. [4] formulates an MICP based on piecewise linear paths, accounting for constraint satisfaction between time steps. [4] is a significant source of inspiration for us, and our use of Bezier splines to represent smooth paths is a generalization of this idea. In addition to allowing us to place constraints on the whole path, not just

the sample points, Bezier splines allow us to enforce dynamic feasibility for differentially flat systems, as well as to optimize for quantities like path length, velocity, and acceleration.

As an alternative way to make MICP more efficient, we proposed a formulation with more binary variables but a tighter convex relaxation in [2], resulting in better branch-and-bound solver performance in practice. The results in this paper are a substantial improvement on that basic idea. Our proposed approach results in an MICP with an even tighter convex relaxation: so tight, in fact, that it can be solved with convex optimization and rounding [6]. Interestingly, it is only through connections with older automata-theoretic methods that we are able to formulate this efficiently-solvable MICP. In this sense, we believe that our proposed approach brings together the best of automata-based and MICP-based methods.

Finally, we acknowledge the recent trend of attempting to avoid the NP-hardness of temporal logic motion planning altogether by providing approximate solutions via non-convex optimization [25, 26, 27, 28], learning [29, 30], or control barrier functions [31, 32]. While such approaches can be extremely efficient and may be practical for some applications, they offer limited or no completeness guarantees and rarely scale to very complex specifications like that shown in Fig. 1a.

III. PROBLEM FORMULATION

A. Linear Temporal Logic

In this section, we introduce the basics of LTL. Further details can be found in [8] and [9].

The syntax, or grammar, of LTL is defined as follows:

$$\varphi := \top \mid a \mid \neg\varphi \mid \varphi_1 \wedge \varphi_2 \mid \bigcirc\varphi \mid \varphi_1 \text{U} \varphi_2, \quad (1)$$

where \top denotes “true”, a is an atomic proposition from the set AP , \neg (“not”) is the negation operator, \wedge (“and”) is the conjunction operator, \bigcirc is the “next” temporal operator, and U is the “until” temporal operator. These operators can be combined to form new operators like “or” ($\varphi_1 \vee \varphi_2 = \neg(\neg\varphi_1 \wedge \neg\varphi_2)$), “eventually” ($\diamond\varphi = \top \text{U} \varphi$), and “always” ($\square\varphi = \neg\diamond\neg\varphi$).

The semantics, or meaning, of LTL is defined over sequences of atomic propositions called *words*:

Definition 1. A word $\sigma = A_0, A_1, A_2, \dots$ is a sequence of atomic propositions, where $A_i \in 2^{AP}$ is a set of atomic propositions. We denote the suffix beginning at index j as $\sigma[j \dots] = A_j, A_{j+1}, \dots$

With this in mind, LTL semantics are defined recursively as follows, where we denote the fact that a word σ satisfies an LTL formula φ with $\sigma \models \varphi$:

- $\sigma[j \dots] \models \top$.
- $\sigma[j \dots] \models a$ if and only if $a \in A_j$.

- $\sigma[j \dots] \models \varphi_1 \wedge \varphi_2$ if and only if $\sigma[j \dots] \models \varphi_1$ and $\sigma[j \dots] \models \varphi_2$.
- $\sigma[j \dots] \models \neg\varphi$ if and only if $\sigma[j \dots] \not\models \varphi$.
- $\sigma[j \dots] \models \bigcirc\varphi$ if and only if $\sigma[j+1 \dots] \models \varphi$.
- $\sigma[j \dots] \models \varphi_1 \text{U} \varphi_2$ if and only if $\exists k \geq j$ such that $\sigma[k \dots] \models \varphi_2$ and $\sigma[i \dots] \models \varphi_1$ for all $j \leq i < k$.

Full LTL, as defined above, is evaluated on infinite length words $\sigma \in (2^{AP})^\omega$. An important subset, or fragment, of LTL is the set of *syntactically co-safe* formulas:

$$\varphi := \top \mid a \mid \neg a \mid \varphi_1 \wedge \varphi_2 \mid \varphi_1 \vee \varphi_2 \mid \bigcirc\varphi \mid \varphi_1 \text{U} \varphi_2. \quad (2)$$

Satisfaction of such a co-safe formula can be uniquely determined by a finite-length word. This fragment is of particular interest for motion planning problems, since most motion plans are of finite length. Infinite words can be relevant to motion planning, however, if plans contain loops: for example, $\varphi = \square\diamond a$ might specify that a robot must visit a recharging station labeled “ a ” infinitely often. In this paper, we present motion planning algorithms for both the co-safe fragment and full LTL, though we are able to provide the strongest completeness and optimality guarantees only for co-safe formulas.

The final aspect of LTL that we will highlight here is its relationship with automata. In short, any LTL formula can be transformed into a Deterministic Buchi Automaton (DBA), and any co-safe LTL formula can be transformed into a Deterministic Finite Automaton (DFA). These are defined as follows:

Definition 2. An deterministic automaton is a tuple $\mathcal{A} = (Q, q_0, \Sigma, \delta, F)$, where

- Q is a set of states,
- $q_0 \in Q$ is an initial state,
- Σ is an input alphabet,
- $\delta : Q \times \Sigma \rightarrow Q$ are transition relations
- $F \subseteq Q$ is a set of accepting states

If \mathcal{A} is a DFA, any accepting run must end at a state in F . If \mathcal{A} is a DBA, any accepting run must visit F infinitely often.

An example of an LTL formula and a corresponding automaton is shown in Figure 4. Only those words that satisfy the LTL formula are accepted as inputs to the automaton. The initial state is (1), while the accepting state (2) is marked with a double circle.

Details of the conversion process between LTL and DFA/DBA can be found in [9, 8]. While the worst-case complexity for this conversion is double-exponential in the size of the LTL formula, mature model-checking software is available which can perform the conversion fairly rapidly for modestly sized formulas [8, 33, 34].

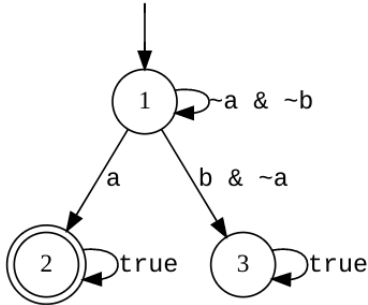


Fig. 4: An automaton corresponding to the LTL formula $\varphi = \neg b U a$, generated by the LTLf2DFA tool [33].

B. LTL Motion Planning

To apply LTL formulas to motion planning, we assume that a set of labeled convex sets in the robot’s configuration space is given. More formally, we use \mathcal{X} to denote a set of convex regions of the robot’s configuration space, $\mathcal{X}_i \subseteq \mathbb{R}^n$. We also define $L : \mathcal{X} \rightarrow 2^{AP}$ as the mapping from these regions to a set of atomic propositions. The label $L(\mathcal{X}_i)$ indicates which atomic propositions hold in region \mathcal{X}_i . This label applies to every configuration in \mathcal{X}_i . It is possible that no atomic propositions hold at a given region, i.e., $L(\mathcal{X}_i) = \emptyset$, and the regions may or may not overlap. Additionally, the set of labeled regions need not cover the entire configuration space.

Informally, our goal is to find a path in configuration space that satisfies a given specification. More formally, we define LTL satisfaction for a path as follows:

Definition 3. A path $p : \mathbb{R}^+ \rightarrow \mathbb{R}^n$ is a mapping from time $t \in \mathbb{R}^+$ to configuration¹ $q \in \mathbb{R}^n$, such that $q_t = p(t)$ is the system configuration at time t .

Definition 4. The trace of path p is the sequence of labels $L(\mathcal{X}_i)$ associated with the regions \mathcal{X}_i visited by p , i.e., $\text{trace}(p) = L(\mathcal{X}_0), L(\mathcal{X}_1), \dots$

In this way, we can say that a path p satisfies a specification φ if $\text{trace}(p) \models \varphi$.

C. Problem

With this notion of path satisfaction in mind, we present a formal problem statement as follows:

Problem 1. Given an initial configuration q_0 , convex regions \mathcal{X} , labels L , and an LTL specification φ , find a

¹Systems where the configuration space is not \mathbb{R}^n could be considered if we represent paths with generalized Bezier splines [35, 36]. It is often the case for differentially flat systems, however, that even if the configuration space is non-Euclidean, flat outputs are in \mathbb{R}^n [19].

minimum-cost path that satisfies the specification, i.e.,

$$\min_p J(p) \quad (3a)$$

$$\text{s.t. } \text{trace}(p) \models \varphi, \quad (3b)$$

$$p \in \mathcal{C}^d, \quad d \geq 0, \quad (3c)$$

$$p(0) = q_0. \quad (3d)$$

The cost J can be any convex function of the path p or its time derivatives. For example, it might be desirable to minimize path length or snap (second derivative of acceleration) [37]. A variety of costs which are convex in our parameterization of p are discussed in Section V-A. The constraint $p \in \mathcal{C}^d$ ensures d -times continuous differentiability, allowing us to enforce dynamical feasibility for any differentially flat system [19].

IV. BACKGROUND

A. Bezier Curves

To solve the optimization problem (3) numerically, we need to somehow represent the continuous path p with a finite set of points. The standard approach in the temporal logic literature is to discretize the path, considering its value only at regularly spaced sample points [1]. But, as discussed in Section II, this sort of discretization leads to clipping and pass-through problems.

In this paper, we parameterize the path p with a sequence of Bezier curves (i.e., a Bezier spline). A Bezier curve $b : [0, 1] \rightarrow \mathbb{R}^n$ is defined by

$$b(s) = \sum_{i=0}^k \binom{k}{i} (1-s)^{k-i} s^i \gamma_i, \quad (4)$$

where k is the order and $\gamma_i \in \mathbb{R}^n$ are the $k+1$ control points. Note that piecewise linear paths, such as those considered in [4], are a special case where $k=1$.

Bezier curves have numerous appealing properties, and indeed they have been widely used in the robotic motion planning literature [38], though they are less common in the context of temporal logic:

- A Bezier curve of order k is differentiable $k-1$ times.
- The time derivative of a Bezier curve is another Bezier curve.
- Bezier curves can be lined up to form a path (spline) by placing constraints on their control points, i.e., the last control point of the previous segment must be equal to the first control point of the next segment. Similar constraints can be applied to enforce a desired degree of differentiability.
- A Bezier curve is contained in the convex hull of its control points.

Figures 2, 3, and 7 show such Bezier splines. Control points are illustrated with red dots connected by dotted lines, while the path is shown in solid blue.

B. Graphs of Convex Sets

The computational workhorse behind our proposed approach is Graphs of Convex Sets (GCS), a framework first introduced in [5] and applied to standard motion planning problems (reach a goal and avoid obstacles) in [6]. In this work, we are heavily inspired by [6], and show that the promising computational attributes of GCS can be applied to motion planning problems much more complex than the classical reach-avoid problem. In particular, we show that LTL motion planning can be cast as a shortest path problem in a GCS, which can be solved efficiently using tools developed in [5, 6].

In short, the GCS framework aims to find the shortest path in a graph, where each vertex of the graph is associated with a convex set, and path lengths depend on which point in the set is chosen. A simple illustration can be found in [5, Fig. 1]. More formally, a GCS is defined as follows:

Definition 5. A Graph of Convex Sets $\mathcal{G} = (\mathcal{V}, \mathcal{E})$ is a directed graph where

- \mathcal{V} is a set of vertices,
- Each vertex $v \in \mathcal{V}$ is associated with a convex set \mathcal{X}_v and a point $x_v \in \mathcal{X}_v$,
- $\mathcal{E} \subset \mathcal{V} \times \mathcal{V}$ is a set of edges,
- Each edge $e = (u, v) \in \mathcal{E}$ is associated with a convex non-negative length function $l_e(x_u, x_v)$ and (optionally) a convex constraint $(x_u, x_v) \in \mathcal{X}_e$.

Given a GCS, the goal is to find a minimum-cost path from a source vertex $v_0 \in \mathcal{V}$ to a target vertex $v_T \in \mathcal{V}$. Defining a path ξ as a sequence of vertices, denoting the set of all paths that connect v_0 and v_T as Ξ , and denoting as \mathcal{E}_ξ the set of edges traversed by path ξ , we can state this problem formally as follows:

$$\min \sum_{e=(u,v) \in \mathcal{E}_\xi} l_e(x_u, x_v) \quad (5a)$$

$$\text{s.t. } \xi \in \Xi \quad (5b)$$

$$x_v \in \mathcal{X}_v \quad \forall v \in p \quad (5c)$$

$$(x_u, x_v) \in \mathcal{X}_e \quad \forall e = (u, v) \in \mathcal{E}_\xi. \quad (5d)$$

This problem turns out to be NP-hard in general, and but an efficient MICP encoding (using perspective functions and harnessing graph-theoretic connections) was proposed in [5]. This MICP has a very tight convex relaxation, meaning it is fairly close to convex optimization and tends to be efficiently solved by branch-and-bound solvers. The convex relaxation is so tight, in fact, that good solutions can often be found with a combination of convex optimization and rounding [6]. When convex optimization is used in this way, it is possible to bound the optimality gap without solving a full MICP [6, Section 4.2], and convex optimization is

often able to find a globally optimal solution—such is the case with the example in Fig. 1a.

While there are many important details in the transcription of problem (5) into a convex program, we refer the interested reader to [5, 6] for these details. In this paper, we use the GCS tools provided in Drake [39]. With that in mind, our primary contribution is to show that Problem 1 can be rewritten as a GCS problem of the form (5): then existing tools can be used to solve (5) rapidly with convex programming.

V. LTL MOTION PLANNING AS A GRAPH OF CONVEX SETS

In this section, we present our main results on transforming an LTL motion planning problem into a GCS problem. Once we have a GCS problem of the form (5), we can solve (5) exactly using MICP or approximately using convex optimization and rounding.

In Section V-A we consider co-safe LTL formulas, a fragment which includes most specifications relevant to motion planning. In Section V-B we extend these result to full LTL formulas, considering infinite-length paths via loops.

A. Co-Safe Formulas

The basic idea, outlined in Algorithm 1, is as follows: first we construct a finite transition-system abstraction and convert the given co-safe LTL formula into a DFA. We then construct a graph of convex sets as the product of the transition system and the DFA. The shortest path in this product GCS corresponds to a minimum-cost path that satisfies the LTL specification.

Algorithm 1 Co-Safe LTL Motion Planning

Require: spec φ , regions \mathcal{X} , labels L , initial state q_0
 $TS = \text{TransitionSystem}(\mathcal{X}, L)$ ▷ Def. 6
 $\mathcal{A} = \text{DFA}(\varphi)$
 $\mathcal{G} = TS \otimes \mathcal{A}$ ▷ Def. 7
 $p^* = \text{shortest path in } \mathcal{G}$ ▷ MICP or convex opt.
return p^*

This procedure is very similar to, and indeed heavily inspired by, classical model checking approaches that also take a product between a DFA and a transition system, then perform graph search to certify satisfaction [8]. The key difference in this case is that the physical layout of the scenario and constraints on the continuous path are included in the product graph, which is a GCS. Existing automata-based LTL motion planning methods return a sequence of regions from graph search, and an additional low-level planner is needed to find a continuous path consistent with this sequence of regions [3, 10, 11]. Our approach, on the other hand, combines

the automata-based handling of logical constraints and optimization-based consideration of a continuous path in one step, via the GCS framework.

First, we construct a transition system from the given labeled convex regions as follows:

Definition 6. *The transition system abstraction is a tuple $TS = (S, s_0, \rightarrow, \mathcal{L}, \mathcal{P})$, where*

- S is a set of states corresponding to each region,
- $\mathcal{P} : S \rightarrow \mathcal{X}$ is a mapping from states to convex sets in configuration space,
- s_0 is an initial state such that $q_0 \in \mathcal{P}(s_0)$,
- \rightarrow is a transition relation, where $s \rightarrow s'$ if and only if $\mathcal{P}(s) \cap \mathcal{P}(s') \neq \emptyset$,
- $\mathcal{L} : S \rightarrow 2^{AP}$ is a labeling function, $\mathcal{L}(s) = L(\mathcal{P}(s))$.

Note that we define a transition whenever there is a non-empty intersection between regions. Intersecting regions may have significant overlap, or may simply be adjacent to one another.

To transform the LTL formula φ into a DFA \mathcal{A} , we can use any one of a variety of existing software tools. In the examples of Section VII, we use the LTLf2DFA tool [33]. Further details on this conversion procedure can be found in [8, 9].

The final step is to formulate a GCS as the product of TS and \mathcal{A} :

Definition 7. *The product $\mathcal{G} = TS \otimes \mathcal{A}$ is a GCS as follows:*

- $\mathcal{V} = \{S \times Q, v_T\}$ are the vertices,
- $v_0 = (s_0, q_0)$,
- v_T is an extra vertex, where edges $(s, q) \rightarrow v_T$ exist only if $q \in F$,
- other edges in \mathcal{E} are such that $(s, q) \rightarrow (s', q')$ exists if and only if $s \rightarrow s'$ is a transition in TS , and $\delta(q, \mathcal{L}(s)) = q'$ is a transition in \mathcal{A} ,
- $\mathcal{X}_v = \mathcal{P}(s)^{k+1}$, where k is the desired Bezier curve degree and \mathcal{Y}^k denotes the Cartesian power of convex set \mathcal{Y} ,
- $x_v = [(\gamma_0^v)^T, (\gamma_1^v)^T, \dots, (\gamma_k^v)^T]^T$ are Bezier curve control points associated with vertex v ,
- \mathcal{X}_e are defined such that $\gamma_k^u = \gamma_0^v$, ensuring continuity of adjacent Bezier curves. Similar constraints are applied to control points for the derivatives of the Bezier curve, up to a desired degree of smoothness.

The basic idea is to define a vertex for each unique pair of states in the DFA and the TS. Edges connect vertices only if corresponding edges exist in both the DFA and the TS: this ensures that both the physical constraints of the scenario and the logical constraints from the LTL formula are met. The target state v_T is defined such that any path to v_T must first pass through an accepting state

(F) of the DFA, enforcing satisfaction of the formula. The convex set \mathcal{X}_v for each vertex corresponds to a convex region. The continuous variables $x_v \in \mathcal{X}_v$ are the control points of a Bezier curve that is constrained to lie within the corresponding region. Edge constraints \mathcal{X}_e ensure that control points of adjacent states line up, forming a continuous and smooth path.

Defined in this way, any path from v_0 to v_T in the GCS \mathcal{G} corresponds to a smooth Bezier spline in configuration space, and is guaranteed to satisfy the given co-safe LTL specification.

The last step is to define edge lengths $l_e(x_u, x_v)$, which corresponds to setting the path cost $J(p)$ in (3). While any convex function could be used, an approximation of the Bezier curve length such as

$$l_e(x_u, x_v) = \sum_{i=0}^k \|\gamma_i^u - \gamma_{i+1}^u\| \quad (6)$$

is particularly appealing. If $\|\cdot\|$ is chosen to be the L2 norm, then $J(p)$ is a strict overapproximation of the actual path length, with the approximation typically growing tighter the more control points are used. For very large-scale problems, it may be more appealing to choose $\|\cdot\|$ as the L1 norm. While this gives a looser approximation of the path length, the resulting convex programs are Linear Programs (LPs) rather than Second Order Cone Programs (SOCPs) [5], for which numerical solvers are more mature and scalability can be improved. Since the derivative of a Bezier curve is another Bezier curve, a similar procedure can be applied to add cost terms related to the time derivatives of the path.

B. Full LTL

To consider full LTL specifications, we need to somehow reason about infinite-length paths with a finite number of decision variables. Again inspired by the model checking literature, we choose to represent such infinite paths with loops [9], e.g.,

$$\sigma = A_0, A_1, \dots, A_k, (B_0, B_1, \dots, B_l)^\omega. \quad (7)$$

This representation allows us to consider infinite behavior by searching for two finite paths: a prefix that is executed once and a suffix that repeats forever.

Much of the machinery developed in Section V-A above can be applied directly to the full LTL case. We can similarly define a transition system TS , convert the LTL formula φ into a DBA (rather than a DFA) \mathcal{A}_B , and compute a GCS as the product $\mathcal{G} = TS \otimes \mathcal{A}_B$.

The key difference is the acceptance condition for a DBA. For a DBA, it is not sufficient to simply reach an accepting state: we must both reach an accepting state and find a loop that visits the accepting state infinitely

often. This loop corresponds to the second finite path, with trace B_0, B_1, \dots, B_l .

We address this problem by breaking down the solution into two separate GCS solves. This procedure is outlined in Algorithm 2. The first solve is identical to the procedure for co-safe formulas outlined above: we simply find a path from the initial state to an accepting state. The trace of this path is the first finite word A_0, A_1, \dots, A_k . The second GCS solve looks for a loop that starts and ends with the same Bezier curve segment as the first solve. The trace of this loop corresponds to the repeated finite word B_0, B_1, \dots, B_l . Concatenating these two paths provides an infinite-length path with a loop that satisfies the specification.

Algorithm 2 Full LTL Motion Planning

Require: spec φ , regions \mathcal{X} , labels L , initial state q_0
 $TS = \text{TransitionSystem}(\mathcal{X}, L)$
 $\mathcal{A}_B = \text{DBA}(\varphi)$
 $\mathcal{G} = TS \otimes \mathcal{A}_B$
while \mathcal{G} contains accepting states **do**
 $p_1 =$ shortest path in \mathcal{G} from v_0 to v_T
 $v_F = (s_F, q_F), q_F \in F$ is accepting state from p_1
 $p_2 =$ shortest path in \mathcal{G} from v_F to v_F
if $p_2 \neq \emptyset$ **then**
 return $p^* = p_1 \cdot p_2$
else
 $\mathcal{G}.pop(v_F)$ \triangleright Remove v_F and try again
end if
end while
return no solution found

It may be possible that the first GCS solve returns a path from which no loops are possible, even though another initial path might admit a valid loop. In this case, we take a CEGIS-inspired approach, discarding the accepting state used in the first GCS solve and attempting to re-solve the problem. As explored in further detail in Section VI, this procedure comes with less satisfying formal guarantees than the procedure for co-safe formulas.

Nonetheless, this two-step procedure is able to find solutions for full LTL specifications like that shown in Fig. 5. In that example, the specification

$$\varphi = \square(\diamond a \wedge \diamond b) \quad (8)$$

requires a mobile robot to visit two regions infinitely often. The first segment, p_1 , drives the robot to visit regions a and b , reaching an accepting state of the automaton \mathcal{A}_B . The second segment, p_2 , forms a loop and lines up with p_1 in region b .

VI. THEORETICAL ANALYSIS

In this section, we provide a formal analysis of the soundness, completeness, and computational complexity

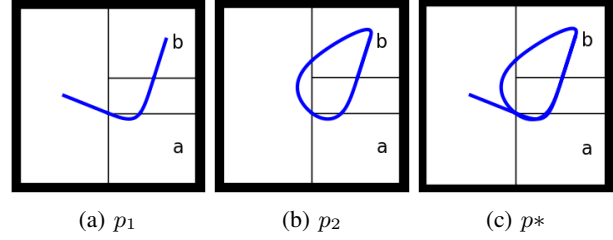


Fig. 5: A solution to the LTL specification (8), which requires the robot to visit both regions a and b infinitely often, and is not part of the co-safe fragment.

of our proposed approach. In short, our method is sound and complete for co-safe LTL formulas, sound for general LTL formulas, has double exponential complexity in the formula size, polynomial complexity in the number of control points, and polynomial complexity in the configuration space dimension.

In all of this analysis, there are four cases to consider, since we can have co-safe or general LTL formulas, and we can solve the GCS problem with either MICP or convex optimization and rounding.

A. Soundness

In this section we consider soundness. An LTL motion planner is sound if every motion plan returned by the planner satisfies the given specification.

Soundness is a relatively easy property to ensure, and our proposed approach is sound regardless of whether co-safe or full LTL formulas are used, and regardless of whether the GCS problem is solved with MICP or convex optimization.

Theorem 1 (Soundness for co-safe LTL formulas). *If Algorithm 1 returns a non-empty path p for co-safe LTL specification φ , then $\text{trace}(p) \models \varphi$.*

Proof. By construction of the GCS \mathcal{G} (Def. 7), any path in \mathcal{G} that reaches the target vertex v_T corresponds to a path in the DFA \mathcal{A} that reaches an accepting state $q_F \in F$. By the relationship between LTL formula φ and the DFA \mathcal{A} , this means that the continuous path p travels through a sequence of regions such that the corresponding sequence of labels satisfies φ . Thus the theorem holds, regardless of whether MICP or convex programming is used to find such a path. \square

Theorem 2 (Soundness for full LTL formulas). *If Algorithm 2 returns a non-empty path p given LTL specification φ , then $\text{trace}(p) \models \varphi$.*

Proof. By construction of the GCS \mathcal{G} , any solution to the two-step procedure of Algorithm 2 corresponds to a path that reaches an accepting state $q_F \in F$ in the DBA \mathcal{A}_B and loops back to q_F . Therefore the path visits

F infinitely often, satisfying the specification. Thus the theorem holds, regardless of whether MICP or convex programming is used to find such a path. \square

It is worth noting that these soundness properties apply to the whole path p , not just predefined sample points. This is a notable improvement over much prior work on temporal logic motion planning in discrete time [1, 8], where clipping between time samples might falsify the specification (e.g., lead to a collision with obstacles). Our method guarantees that each Bezier curve segment is completely contained in a single region, eliminating this soundness gap.

B. Completeness

In this section we consider the completeness of Algorithms 1 and 2. An LTL motion planner is complete if it always finds a solution when one is available. The completeness guarantees in this section are posed over a given set of convex regions: optimal decomposition of configuration space into labeled convex regions remains an important area for future research.

We first consider the case of a co-safe LTL specification where MICP is used to solve the GCS subproblem. This case offers the strongest completeness guarantees under relatively modest assumptions:

Theorem 3 (Completeness for co-safe LTL with MICP). *Assume that there exists a satisfying Bezier spline solution of the desired degree and smoothness, and that the control points of each segment are each contained within a single region. If MICP is used to solve the GCS subproblem, then Algorithm 1 will return a path that satisfies the given co-safe LTL specification.*

Proof. By construction of the GCS \mathcal{G} (Def. 7), if a satisfying path exists then there exists a path from v_0 to v_T in \mathcal{G} . This follows from the relationship between the specification φ and the automaton \mathcal{A} . By [5, Theorem 5.6], the MICP used to solve (5) is guaranteed to find the optimal path from v_0 to v_T . \square

The primary assumption required for this theorem merits some discussion. It may be the case that a satisfying path exists, but it cannot be represented by a Bezier spline of the desired degree and smoothness. It could also be the case that a Bezier spline solution exists, but requires control points that lie outside a region. In either of these cases, Algorithm 1 may fail to find a solution even though one exists.

Fortunately, there is a simple practical fix to this problem: increase the number of control points, and/or reduce the desired smoothness. Increasing the number of control points adds additional flexibility, and typically brings control points closer to the path. Reducing the

smoothness (e.g. C^1 rather than C^2) eliminates some of the constraints on the control points, and may similarly allow for solutions that were previously unavailable.

In the case of co-safe LTL specifications where convex optimization and rounding are used to solve the GCS subproblem, we can certify probabilistic completeness:

Theorem 4 (Completeness for co-safe LTL with Convex Optimization). *Assume that there exists a satisfying path made up of Bezier curve segments of desired degree and continuity, and that the control points of each segment are contained within a single region. Furthermore, assume that the convex relaxation of the GCS subproblem assigns nonzero values to binary variables on the optimal path. If the convex optimization and rounding scheme described in [6] is used to solve the GCS subproblem, then Algorithm 1 will return a path p that satisfies the given co-safe LTL specification with probability 1 as the number of rounding iterations approaches infinity.*

Proof. By construction of the GCS \mathcal{G} (Def. 7), if a satisfying path exists then there exists a path from v_0 to v_T in \mathcal{G} . This follows from the relationship between the specification φ and the automaton \mathcal{A} . The rounding scheme described in [6, Section 4.2] treats the values of binary variables from the convex relaxation as probabilities, and performs rounding as a randomized depth-first search with backtracking. As the number of rounding iterations approaches infinity, this procedure will eventually explore all possible paths in \mathcal{G} with probability 1. If the convex relaxation of (5) is not feasible, then the MICP is not feasible and no solution exists (by Theorem 3). \square

Remark 1. *The assumption of nonzero values for binary variables on the optimal path is minimally restrictive in practice. In fact, branch-and-bound MICP solvers often prune branches based on integer-valued binary variables in the convex relaxation [40].*

In practice (see the examples in Section VII), the gap between convex optimization and MICP is quite small. For all of the examples considered in this paper, convex optimization was able to find a satisfying solution—if not a certified globally optimal solution—with only a few (< 10) rounding iterations.

For full-LTL specifications, the necessity of finding a loop makes any completeness guarantees significantly more limited. Nonetheless, we can guarantee completeness under a set of more restrictive assumptions:

Theorem 5. *Assume that the conditions for Theorem 3 hold. Furthermore, assume that for at least one accepting state $v = (s, q), q \in F$ in the GCS \mathcal{G} , every Bezier curve b contained in X_v admits a loop through \mathcal{G} that*

starts and ends with b . Then Algorithm 2 will return a satisfying path.

Proof. By Theorem 3, Algorithm 2 will eventually find a path p_1 that reaches the special accepting state v . If Algorithm 2 finds a path p_1 to an accepting state v' that does not admit a loop for every Bezier curve in $X_{v'}$, then v' will be removed from the graph and a new p_1 computed. Once a suitable p_1 is found, a loop p_2 is similarly guaranteed to be found by Theorem 3 and the assumption that a loop exists. The complete path $p^* = p_1 \cdot p_2$ corresponds to visiting the accepting set F infinitely often, thus the Theorem holds. \square

Probabilistic completeness guarantees can be obtained for the full LTL case when convex optimization is used instead of MICP, following similar reasoning to Theorem 4.

The extra assumption that every Bezier curve in at least one accepting state admit a loop is needed to ensure that the CEGIS-inspired procedure in Algorithm 2 eventually returns a solution. The assumption that every Bezier curve admit a loop is particularly restrictive—it may be the case that a loop (p_2) is possible, but not from the starting Bezier curve segment that ends p_1 . This restriction is necessary because the GCS framework does not allow for constraints between continuous variables x_v that are not connected by an edge. This means that to find a loop, we must constrain the initial and final continuous variables x_0 and x_T to some a-priori fixed values.

C. Complexity

In this section, we formally characterize the computational complexity of our proposed approach, focusing on the case where the GCS subproblem is solved with convex optimization and rounding, as described in [6].

At first glance, it may appear that since LTL motion planning is NP-hard, convex optimization is solvable in polynomial time, and we solve LTL motion planning with convex optimization, we have shown that $P = NP$. We emphasize that this is not the case for two reasons: first, convex optimization provides only an approximate solution to the GCS subproblem, which is itself NP-hard [5]. Second, and more importantly, the size of the automaton \mathcal{A} is double exponential in the size of the LTL formula φ , resulting in a GCS \mathcal{G} which is also double exponential in the size of the LTL formula.

Theorem 6. *Given the GCS \mathcal{G} , the time complexity of finding an approximate solution to the shortest path problem with convex optimization is $O(2^{2^{|\varphi|}})$, where $|\varphi|$ is the size of φ .*

Proof. The conversion of φ to automaton \mathcal{A} results in an automaton with $O(2^{2^{|\varphi|}})$ states [8], so the GCS \mathcal{G} has

$O(2^{2^{|\varphi|}})$ vertices and edges. The convex optimization encoding of [6] results in an LP or SOCP with variables for each vertex and edge in \mathcal{G} . Since LP and SOCP have polynomial time complexity in the number of decision variables [41], the overall time complexity is $O(2^{2^{|\varphi|}})$. \square

While exponential complexity in the formula size is inevitable due to the NP-hardness of the problem, our proposed approach scales polynomially in a number of variables of practical interest:

Theorem 7. *Given the GCS \mathcal{G} , the time complexity of finding an approximate solution to the shortest path problem with convex optimization is polynomial in k , the degree of each Bezier curve segment.*

Proof. This follows from the fact that the number of decision variables increases linearly with k , and the convex optimization problem is an LP or SOCP which can be solved in polynomial time with interior point methods [41]. \square

This means that the complexity is polynomial in the total number of control points γ_i used to represent a curve. This is in contrast to standard MICP-based methods, which scale exponentially in the number of sample points used to represent a path. In practice, we find that increasing the number of control points has little practical impact on solve times, see Fig. 6.

Theorem 8. *Given the GCS \mathcal{G} , the time complexity of finding an approximate solution to the shortest path problem with convex optimization is polynomial in n , the dimension of the configuration space.*

Proof. This follows from the fact that the number of decision variables increases linearly with n , and the convex optimization problem is an LP or SOCP which can be solved in polynomial time with interior point methods [41]. \square

This is a key factor in enabling our approach to scale to high-dimensional configurations spaces, as explored in Section VII-C.

VII. EXAMPLES

In this section, we demonstrate the scalability of our proposed approach with several simulation examples. Code for reproducing these examples is available at [7]. All experiments were performed on a laptop with an Intel i7 CPU and 32GB RAM. The underlying convex optimization solver was MOSEK [42], accessed via Drake [39] Python bindings.

Solve times for all of the examples are shown in Table I. In addition to the final solve time, we report the time converting the LTL specification φ to a DFA

\mathcal{A} and time to form the GCS $\mathcal{G} = \mathcal{A} \otimes TS$. Converting LTL to DFA can be particularly expensive for complex specifications due to the double exponential complexity of this operation [8].

Of these steps, only the final solve is an online operation: all other steps can be performed offline and their results reused for different initial conditions. In all of the examples, we use convex optimization rather than MICP to solve the GCS problem.

Name	Fig.	LTL to DFA	Form GCS	Solve
shortest path	3	0.13	0.05	0.34
simple key-door	2	0.54	0.34	0.29
complex key-door	1a	32 min.	547	5.82
multi-target	7	0.64	3.72	7.28
manipulator	9	0.10	0.08	1.09
humanoid	1b	0.11	0.18	7.72

TABLE I: Timing breakdown for each of the examples in this section. Times are in seconds unless otherwise noted. All operations can be performed offline except “Solve”.

A. Planar Motion Planning

In this section, we consider motion planning for a simple planar robot. As we consider path planning rather than trajectory planning, the particular dynamics of the robot are not used. We can, however, design paths with a desired degree of smoothness (see Section IV-A), ensuring feasibility for any differentially flat system [19].

The first example, shown in Fig. 3, illustrates the advantage of considering both logical constraints and scenario geometry at the same time (something that most automata-based methods struggle with). A mobile robot is tasked with eventually reaching one of two target regions, labeled a and b respectively:

$$\varphi = \diamond(a \vee b). \quad (9)$$

An abstraction-based motion planner such as [11] would likely choose the longer path to region a , since this requires fewer transitions in \mathcal{G} . Our planner, on the other hand, finds the shorter path to target b directly.

The cost in this example is a simple penalty on path length (L2 norm of distance between control points). A Bezier curve of order $k = 4$ is used, and C^2 continuity is enforced. Bezier control points are shown as red dots in Fig. 3, while the final path itself is in blue.

In the second planar motion example, illustrated in Fig. 2, the robot must pick up two keys (i.e., visit green regions labeled $key1$ and $key2$) in order to pass through corresponding doors (red, labeled $door1$ and $door2$) before eventually reaching a goal (blue, labeled $goal$). More formally, this specification can be written as an LTL formula

$$\varphi = (\neg door1 U key1) \wedge (\neg door2 U key2) \wedge \diamond goal. \quad (10)$$

A more complicated version of this specification with five keys and five doors is shown in Fig. 1a. This benchmark example was first proposed in [3], where it was solved with an abstraction-based approach, though no solve times were reported. To the best of our knowledge, the fastest reported solve time for this benchmark is 49.5 seconds from [4]. [4] finds a piecewise linear path (avoiding clipping and pass-through) with MICP. Our proposed approach is roughly an order of magnitude faster (Table I), provided conversion from LTL to DFA and construction of the GCS is performed offline. Furthermore, the path generated with our approach is twice continuously differentiable and certified globally optimal. The extremely long time to convert from LTL to DFA is indicative of the double-exponential complexity of this operation [8].

We use the simpler key-door example (with two doors) to compare with standard MICP-based temporal logic motion planners, which consider a discretization of time rather than continuous-valued curves for motion planning. In particular, we compare with the MICP approach of [20] as implemented in the *stlpy* [24] python library².

The standard MICP represents continuous paths with a pre-specified number of time steps. If too few time steps are used, clipping and pass-through problems can cause the path to intersect with obstacles between time steps, as illustrated in Fig. 2a. Our proposed approach, on the other hand, considers the whole curve, and therefore does not suffer from clipping or pass-through even if relatively few control points are used, as shown in Fig. 2b.

Typically, clipping and pass-through are addressed by sampling the path more finely, using more time steps. Unfortunately, this leads to an exponential blowup in time-complexity for the standard approach. Our approach, on the other hand, scales only polynomially with the number of control points (Theorem 7). The practical impact of this fact is illustrated in Fig. 6.

In Fig. 6, we compare solve times for the standard MICP and our proposed approach, varying the number of time steps for the standard approach and the total number of control points used (the rough equivalent of time steps) for our method. Solve times for the standard MICP increase exponentially, as expected: using more than about 30 timesteps is impractical for this specification. Solve times for our proposed approach, on the other hand, stay roughly constant as the total number of control points increases. We can use as many as 90 control points—10 per Bezier curve segment in this example—with minimal impact on solve time.

Our final planar motion planning example, illustrated in Fig. 7, showcases a more complex scenario as well as

²While this library is for STL rather than LTL, the specification in question does not have active timing constraints, rendering the STL and LTL specifications equivalent.

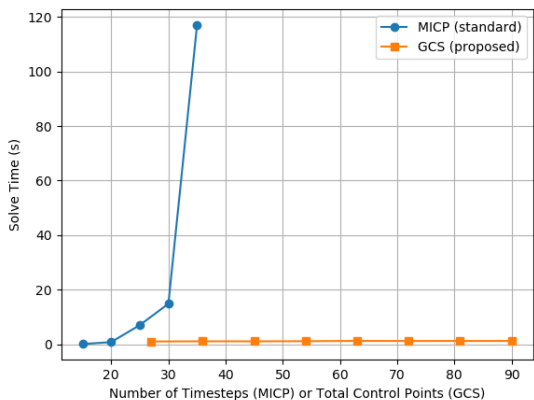


Fig. 6: Plot of solve times as the number of sample points used to represent a path (number of timesteps for a standard MICP, number of control points for our approach) increases. The standard approach scales exponentially in the number of time steps, while solve times for our proposed approach are nearly constant as the number of control points grows.

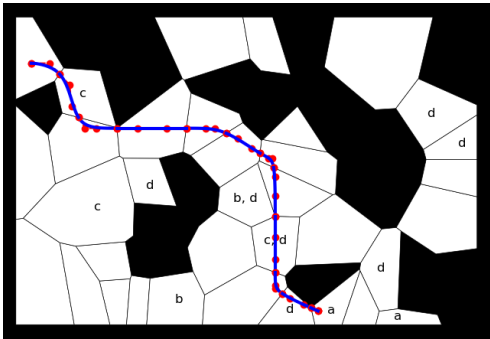


Fig. 7: A mobile robot must navigate an environment with multiple labeled targets, eventually reaching a , c , and d , but always avoiding b . This is formalized by specification (11).

a specification that is not part of the co-safe fragment. The robot is tasked with eventually visiting regions labeled a , c , and d , while always avoiding b :

$$\varphi = \diamond a \wedge \square \neg b \wedge \diamond c \wedge \diamond d. \quad (11)$$

The always operator (\square) means that this specification is not syntactically co-safe [8]. The final loop which renders infinite-length behaviors is trivial, however: the robot simply remains at the final configuration.

The GCS for this multi-target example is relatively large, and the shortest-path subproblem is a large and possibly poorly conditioned SOCP if an L2 norm approximation of the path length is used. We found that MOSEK [42] was unable to converge to a solution to

the SOCP in this case, returning an `Solver Status: UNKNOWN` error code. To avoid this, we used an L1 norm approximation of the path length (see Section V-A) instead. This leads to a LP rather than a SOCP, for which solvers are more mature and reliable. With this L1/LP formulation, MOSEK finds the solution shown in Fig. 7.

B. Comparison with Sampling-Based Motion Planning

For simple reach-avoid problems (a special case of LTL motion planning), GCS-based motion planning was shown to outperform sampling-based methods in [6]. In this section, we explore whether similar advantages hold for motion planning under LTL specifications.

We compare our proposed approach with the state-of-the-art sampling-based planner described in [14]. This method is especially appealing because it does not require computing the product of a transition system and the specification automaton, but rather incrementally builds trees to explore the state-space of the product without constructing it explicitly.

In particular, we consider the example in [14, Section VII.A.]. This example ([14, Fig. 6]) has with six regions of interest (r_i) and two obstacles (obs). The task is specified by the LTL formula

$$\begin{aligned} \varphi = & \diamond(r_1 \wedge \diamond r_3) \wedge (\neg r_1 U r_2) \wedge \\ & \diamond(r_5 \wedge \diamond(r_6 \wedge \diamond r_4)) \wedge (\neg r_4 U r_5) \wedge \square \neg obs. \end{aligned} \quad (12)$$

This specification requires a mobile robot to do the following: eventually visit region r_1 , then r_3 ; not visit r_1 until visiting r_2 ; eventually visit r_5 , r_6 , and r_4 in that order; not visit r_4 before r_5 ; and avoid obstacles.

To compare our approach and [14], we randomly generated 100 initial positions and solved the motion planning problem using our approach and sampling-based planning. For the sampling-based planner we used a maximum of $n_{max} = 1000$ iterations and default parameters from the implementation provided with [14]. For our approach, we solved for a first order Bezier spline with an L2 norm penalty on path length and performed a single rounding iteration. A histogram of solve times is shown in Fig. 8. For both approaches, we exclude the time needed to construct an automaton, as this can be performed offline.

Solve times for our proposed approach were both faster on average (mean of 0.30 vs 0.69 seconds) and more consistent (standard deviation of 0.024 vs 0.52 seconds) than the sampling based approach, though there were some initial conditions for which the sampling-based method found a solution faster.

C. High-DoF Systems

Our proposed approach scales well to high-dimensional configuration spaces. To demonstrate this,

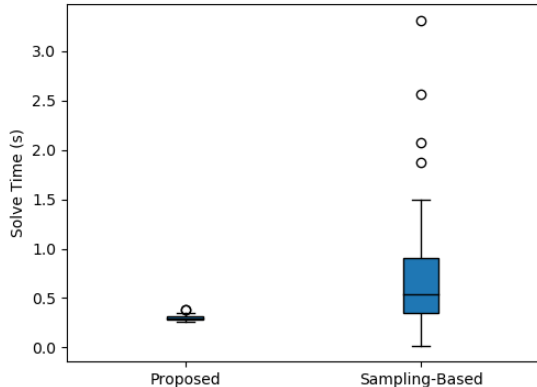


Fig. 8: Solve times for specification (12) using our proposed approach and a sampling-based approach [14] over 100 trials with different initial conditions.

we consider the 7-DoF model of a Franka Panda arm shown in Fig. 9 and the 30-DoF model of an Atlas humanoid shown in Fig. 10. Both models are from Drake [39].

1) *7-DoF Manipulator*: The arm is tasked reaching a target configuration that places its end-effector through a doorway (red box), but it must press a button (blue half circle) before passing through the doorway. This specification can be written as

$$\varphi = \diamond target \wedge \neg doorway U button. \quad (13)$$

Labeled collision-free convex polytopes in configuration space were generated using C-IRIS [43], as implemented in Drake [39].

Our proposed approach offers considerable performance improvements over state-of-the-art methods for temporal logic motion planning in large configuration spaces. In prior work [28], we showed how non-convex trajectory optimization could be used to solve temporal logic motion planning for a similar 7-DoF robot arm, and solved a relatively simple specification ($\diamond(a \vee b)$) in 160 seconds. In contrast, the considerably more complex specification (13) is solved by our proposed approach in about a second.

2) *30-DoF Humanoid*: The Atlas humanoid is tasked with reaching three target boxes, shown in green, blue, and red in Fig. 1b. We use inverse kinematics and C-IRIS [43] to define labeled convex regions of configuration space corresponding to (a) the left hand touching the green target, (b) the right foot touching the red target, and (c) the right hand touching the blue target. We also define an unlabeled convex region without kinematic constraints (d). Seed configurations used to generate these convex sets are shown in Fig. 10.

The specification is then given by

$$\varphi = \diamond(a \wedge \diamond(b \wedge \diamond(c))), \quad (14)$$

which states that the robot should eventually reach targets a , b , and c , in that order.

We fix the pose of the pelvis in the world frame, and do not consider contact interactions with the ground. Balance, contact wrench cone, or other dynamic feasibility constraints are not considered: our goal is merely to find a configuration space path that satisfies the specification. Without a floating base, this is a 30-DoF system.

We search for a satisfying path using Bezier splines of degree $k = 3$ and enforce C^2 smoothness. In addition to an L2 norm penalty on path length, we add a small penalty on configuration space accelerations. As shown in Table I, a locally optimal path is found in 7.72 seconds.

VIII. LIMITATIONS

In this section, we provide a brief overview of the limitations of our proposed approach along with concrete suggestions for mitigating these limitations in practice.

A major drawback is the double-exponential complexity of converting LTL formulas to automata [8]. This limitation is illustrated most clearly in Table I, where conversion to a DFA takes over half an hour for the complex key-door scenario. We performed this conversion using the LTL2DFA python library [33], which uses MONA [34] to perform the underlying conversion. While it is possible that other model checking software (see [8] for a list) might be more performant, any such conversion software will run up against the fundamental double exponential complexity of this conversion.

To mitigate this issue in practice, we note that conversion to an automaton and construction of the GCS can be performed offline if the labeled regions and specification are known a-priori. Any initial condition can be used with this offline-computed GCS: only the initial vertex $v_0 = (s_0, q_0)$ will change. Given a GCS, convex optimization solve times tend to be relatively fast (on the order of seconds), even for specifications where the conversion to an automaton was extremely slow.

A related limitation is the need for labeled convex regions. For simple planar scenarios like those in Section VII-A this may be a reasonable expectation, but for more complex systems with high-dimensional configuration spaces, like the robot arm in Section VII-C, it is not always obvious how to obtain such labeled regions. Fortunately, there has been considerable recent progress in decomposition of free space into convex sets. Algorithms like IRIS [44], and C-IRIS [43], provide iterative procedures for inflating convex regions of free space. Such algorithms provide a convenient means of constructing labeled convex sets for high-dimensional

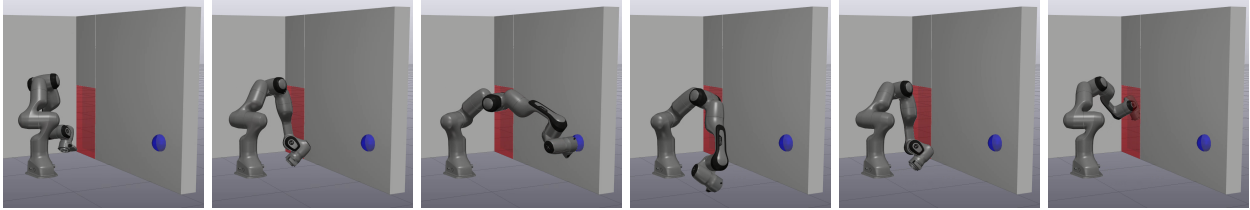


Fig. 9: A 7-DoF manipulator arm is tasked with pushing a button (blue) before reaching through a doorway (red), according to formula (13). A labeled convex decomposition of the configuration space was generated offline using C-IRIS [43].

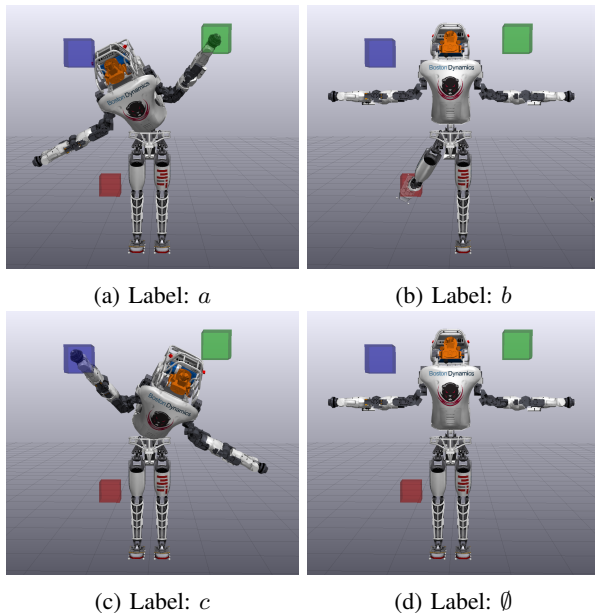


Fig. 10: Seed configurations used to generate labeled convex regions for the Atlas humanoid. For regions labeled a , b , and c , inverse kinematics constraints ensure that the hand or foot stays within the target box.

systems. Efficiently generating convex regions from temporal logic labels directly remains an important area for future research.

Another drawback of this approach is that we consider path planning rather than trajectory planning. This means that satisfying paths do not consider the natural dynamics of the system and may not be dynamically feasible. The ability of Bezier splines to enforce a desired degree of smoothness, however, allows for dynamical feasibility to be enforced for any differentially flat system, a large class of systems that includes quadrotors [37] and differential-drive mobile robots [19].

From a theoretical perspective, the convex optimization approach provides more limited guarantees than MICP, since convex optimization and rounding is not guaranteed to find a globally optimal solution. In prac-

tice, however, this does not appear to be a significant concern. As of the time of writing, we have not come across any examples for which MICP finds a satisfying solution but convex optimization does not.

Finally, we highlight the limited completeness guarantees available for full LTL (non-co-safe) specifications (Theorem 5). This limitation ultimately stems from the difficulty of encoding loop constraints in the GCS framework. Nonetheless, many LTL specifications of practical interest for motion planning either fall within the co-safe fragment (9, 10, 13) or are not syntactically co-safe but have solutions with trivial loops (11).

IX. CONCLUSION AND FUTURE WORK

We presented a convex optimization solution to temporal logic motion planning. The key idea is to convert the LTL motion planning problem into a shortest path problem in a graph of convex sets. This GCS problem can be solved exactly with mixed-integer programming, but also admits a practical approximate solution via convex optimization and rounding [5, 6].

Our proposed approach scales to complex specifications (Fig. 1a) and high-dimensional configuration spaces (Fig. 9), and addresses many of the limitations of standard temporal-logic motion planning methods. We avoid the clipping and pass-through problems associated with discrete-time temporal logic formulations [45] by representing paths with Bezier splines. Unlike standard MICP-based approaches [20, 1, 4], our proposed approach does not scale exponentially with the number of sample points used to represent a path (Fig. 6). Unlike local optimization [25, 26, 27], learning-based [29, 30], or CBF-based [31] approaches, our proposed approach provides probabilistic completeness guarantees under modest assumptions.

Potential areas of future work include extensions to multi-agent and distributed systems, extensions to timed temporal logics like STL and MTL, and use in a model predictive control framework.

REFERENCES

- [1] Calin Belta and Sadra Sadraddini. Formal methods for control synthesis: An optimization perspective. *Annual Review of Control, Robotics, and Autonomous Systems*, 2:115–140, 2019.
- [2] Vince Kurtz and Hai Lin. A more scalable mixed-integer encoding for metric temporal logic. *IEEE Control Systems Letters*, 6:1718–1723, 2021.
- [3] William Vega-Brown and Nicholas Roy. Admissible abstractions for near-optimal task and motion planning. *arXiv preprint arXiv:1806.00805*, 2018.
- [4] Dawei Sun, Jingkai Chen, Sayan Mitra, and Chuchu Fan. Multi-agent motion planning from signal temporal logic specifications. *IEEE Robotics and Automation Letters*, 7(2):3451–3458, 2022.
- [5] Tobia Marcucci, Jack Umenberger, Pablo A Parrilo, and Russ Tedrake. Shortest paths in graphs of convex sets. *arXiv preprint arXiv:2101.11565*, 2021.
- [6] Tobia Marcucci, Mark Petersen, David von Wrangel, and Russ Tedrake. Motion planning around obstacles with convex optimization. *arXiv preprint arXiv:2205.04422*, 2022.
- [7] https://github.com/vincekurtz/ltl_gcs.
- [8] Calin Belta, Boyan Yordanov, and Ebru Aydin Gol. *Formal methods for discrete-time dynamical systems*, volume 15. Springer, 2017.
- [9] Christel Baier and Joost-Pieter Katoen. *Principles of model checking*. MIT Press, 2008.
- [10] Rafael Rodrigues da Silva, Vince Kurtz, and Hai Lin. Active perception and control from temporal logic specifications. *IEEE Control Systems Letters*, 3(4):1068–1073, 2019.
- [11] Rafael Rodrigues da Silva, Vince Kurtz, and Hai Lin. Automatic trajectory synthesis for real-time temporal logic. *IEEE Transactions on Automatic Control*, 67(2):780–794, 2021.
- [12] Edmund Clarke, Orna Grumberg, Somesh Jha, Yuan Lu, and Helmut Veith. Counterexample-guided abstraction refinement. In *International Conference on Computer Aided Verification*, pages 154–169. Springer, 2000.
- [13] Cristian Ioan Vasile and Calin Belta. Sampling-based temporal logic path planning. In *2013 IEEE/RSJ International Conference on Intelligent Robots and Systems*, pages 4817–4822. IEEE, 2013.
- [14] Xusheng Luo, Yiannis Kantaros, and Michael M Zavlanos. An abstraction-free method for multi-robot temporal logic optimal control synthesis. *IEEE Transactions on Robotics*, 37(5):1487–1507, 2021.
- [15] Yiannis Kantaros, Samarth Kalluraya, Qi Jin, and George J Pappas. Perception-based temporal logic planning in uncertain semantic maps. *IEEE Transactions on Robotics*, 2022.
- [16] Liangjun Zhang and Dinesh Manocha. An efficient retraction-based rrt planner. In *2008 IEEE International Conference on Robotics and Automation*, pages 3743–3750. IEEE, 2008.
- [17] Marius Kloetzer and Calin Belta. A fully automated framework for control of linear systems from temporal logic specifications. *IEEE Transactions on Automatic Control*, 53(1):287–297, 2008.
- [18] Hadas Kress-Gazit, Georgios E Fainekos, and George J Pappas. Temporal-logic-based reactive mission and motion planning. *IEEE transactions on robotics*, 25(6):1370–1381, 2009.
- [19] Richard M Murray, Muruhan Rathinam, and Willem Sluis. Differential flatness of mechanical control systems: A catalog of prototype systems. In *ASME International Mechanical Engineering Congress and Exposition*. Citeseer, 1995.
- [20] Vasumathi Raman, Alexandre Donz e, Mehdi Maaoumy, Richard M Murray, Alberto Sangiovanni-Vincentelli, and Sanjit A Seshia. Model predictive control with signal temporal logic specifications. In *53rd IEEE Conference on Decision and Control*, pages 81–87. IEEE, 2014.
- [21] Eric M Wolff, Ufuk Topcu, and Richard M Murray. Optimization-based trajectory generation with linear temporal logic specifications. In *2014 IEEE International Conference on Robotics and Automation (ICRA)*, pages 5319–5325. IEEE, 2014.
- [22] Guang Yang, Calin Belta, and Roberto Tron. Continuous-time signal temporal logic planning with control barrier functions. In *2020 American Control Conference (ACC)*, pages 4612–4618. IEEE, 2020.
- [23] Sadra Sadraddini and Calin Belta. Formal synthesis of control strategies for positive monotone systems. *IEEE Transactions on Automatic Control*, 64(2):480–495, 2018.
- [24] Vincent Kurtz and Hai Lin. Mixed-integer programming for signal temporal logic with fewer binary variables. *IEEE Control Systems Letters*, 6:2635–2640, 2022.
- [25] Yash Vardhan Pant, Houssam Abbas, and Rahul Mangharam. Smooth operator: Control using the smooth robustness of temporal logic. In *2017 IEEE Conference on Control Technology and Applications (CCTA)*, pages 1235–1240. IEEE, 2017.
- [26] Noushin Mehdipour, Cristian-Ioan Vasile, and Calin Belta. Arithmetic-geometric mean robustness for control from signal temporal logic specifications. In *2019 American Control Conference*

- (ACC), pages 1690–1695. IEEE, 2019.
- [27] Yann Gilpin, Vince Kurtz, and Hai Lin. A smooth robustness measure of signal temporal logic for symbolic control. *IEEE Control Systems Letters*, 5(1):241–246, 2020.
- [28] Vince Kurtz and Hai Lin. Trajectory optimization for high-dimensional nonlinear systems under stl specifications. *IEEE Control Systems Letters*, 5(4):1429–1434, 2020.
- [29] Mingyu Cai, Shaoping Xiao, Baoluo Li, Zhiliang Li, and Zhen Kan. Reinforcement learning based temporal logic control with maximum probabilistic satisfaction. In *2021 IEEE International Conference on Robotics and Automation (ICRA)*, pages 806–812. IEEE, 2021.
- [30] K. Leung and M. Pavone. Semi-supervised trajectory-feedback controller synthesis for signal temporal logic specifications. In *American Control Conference, 2022*.
- [31] Lars Lindemann and Dimos V Dimarogonas. Control barrier functions for signal temporal logic tasks. *IEEE control systems letters*, 3(1):96–101, 2018.
- [32] Mohit Srinivasan and Samuel Coogan. Control of mobile robots using barrier functions under temporal logic specifications. *IEEE Transactions on Robotics*, 37(2):363–374, 2020.
- [33] Francesco Fuggitti. Ltlf2dfa, March 2019. <https://doi.org/10.5281/zenodo.3888410>.
- [34] Nils Klarlund and Anders Møller. *MONA Version 1.4 User Manual*. BRICS, Department of Computer Science, University of Aarhus, January 2001. Notes Series NS-01-1. Available from <http://www.brics.dk/mona/>.
- [35] Myoung-Jun Kim, Myung-Soo Kim, and Sung Yong Shin. A general construction scheme for unit quaternion curves with simple high order derivatives. In *Proceedings of the 22nd annual conference on Computer graphics and interactive techniques*, pages 369–376, 1995.
- [36] Zhongxuan Luo, Qian Wang, Xin Fan, Yaqi Gao, and Panpan Shui. Generalized rational bézier curves for the rigid body motion design. *The Visual Computer*, 32(9):1071–1084, 2016.
- [37] Daniel Mellinger and Vijay Kumar. Minimum snap trajectory generation and control for quadrotors. In *2011 IEEE international conference on robotics and automation*, pages 2520–2525. IEEE, 2011.
- [38] Boris Lau, Christoph Sprunk, and Wolfram Burgard. Kinodynamic motion planning for mobile robots using splines. In *2009 IEEE/RSJ International Conference on Intelligent Robots and Systems*, pages 2427–2433. IEEE, 2009.
- [39] Russ Tedrake and the Drake Development Team. Drake: Model-based design and verification for robotics, 2019.
- [40] Michele Conforti, Gérard Cornuéjols, Giacomo Zambelli, et al. *Integer programming*, volume 271. Springer, 2014.
- [41] Yurii Nesterov and Arkadii Nemirovskii. *Interior-point polynomial algorithms in convex programming*. SIAM, 1994.
- [42] MOSEK ApS. *The MOSEK optimization toolbox. Version 9.0.*, 2022.
- [43] Alexandre Amice, Hongkai Dai, Peter Werner, Annan Zhang, and Russ Tedrake. Finding and optimizing certified, collision-free regions in configuration space for robot manipulators. In *International Workshop on the Algorithmic Foundations of Robotics*, pages 328–348. Springer, 2023.
- [44] Robin Deits and Russ Tedrake. Computing large convex regions of obstacle-free space through semidefinite programming. In *Algorithmic foundations of robotics XI*, pages 109–124. Springer, 2015.
- [45] Hai Lin. Mission accomplished: An introduction to formal methods in mobile robot motion planning and control. *Unmanned Systems*, 2(02):201–216, 2014.